Journal of Chromatography B, 879 (2011) 3393–3400

Contents lists available at SciVerse ScienceDirect

Journal of Chromatography B

journal homepage: www.elsevier.com/locate/chromb

Quantitative subproteomic analysis of age-related changes in mouse liver peroxisomes by iTRAQ LC–MS/MS

Hanna Amelina[a,*], Marcus O.D. Sjödin[b], Jonas Bergquist[b], Susana Cristobal[a,c,d]

[a] Department of Biochemistry and Biophysics, Stockholm University, SE-106 91 Stockholm, Sweden
[b] Department of Physical and Analytical Chemistry, Uppsala University, SE-751 24 Uppsala, Sweden
[c] Department of Clinical and Experimental Medicine, Linköping University, SE-581 03 Linköping, Sweden
[d] IKERBASQUE, Basque Foundation for Science, Department of Physiology, University of the Basque Country, Leioa 48940, Spain

ARTICLE INFO

Article history:
Received 15 April 2011
Accepted 26 August 2011
Available online 10 September 2011

Keywords:
Liquid chromatography
Tandem mass spectrometry
Peroxisomes
Aging
Liver
iTRAQ

ABSTRACT

Aging is a complex multifactorial phenomenon, which is believed to result from the accumulation of cellular damage to biological macromolecules. Peroxisomes recently emerged as another important source of reactive oxygen species (ROS) production in addition to mitochondria. However, the role of these organelles in the process of aging is still not clear. The aim of this study was to characterize the changes in protein expression profiles of young (10 weeks old) versus old (18 months old) mouse liver peroxisome-enriched fractions. We have applied shotgun proteomic approach based on liquid chromatography and tandem mass spectrometry (LC–MS/MS) combined with iTRAQ (isobaric tags for relative and absolute quantitation) labeling that allows comparative quantitative multiplex analysis. Our analysis led to identification and quantification of 150 proteins, 8 out of which were differentially expressed between two age groups at a statistically significant level ($p < 0.05$), with folds ranging from 1.2 to 4.1. These proteins involved in peroxisomal β-oxidation, detoxification of xenobiotics and production of ROS. Noteworthy, differences in liver proteome have been observed between as well as within different age groups. In conclusion, our subproteomic quantitative study suggests that mouse liver proteome is sufficiently maintained until certain age.

1. Introduction

Aging is the most complex phenomenon currently known, as it becomes manifest in all organs and tissues, leads to the organism's physiological decline, affects functions at all levels and increases susceptibility to all major chronic diseases. It is a multifactorial process: protein turnover is impaired [1], telomeres shorten [2], somatic mutations increase [3] and chromatin modifications become more and more evident [4]. Nevertheless, aging is still poorly defined at the mechanistic level, even though in recent years much progress has been made by studying genetic mutations altering the life span.

The traditional scientific approach based upon reductionism has not been proved to be particularly efficient in deciphering very complex biological processes. Therefore there was a great promise that aging research would benefit from recently emerged large-scale technology platforms (genomics, transcriptomics, proteomics, metabolomics), which are designed to provide a global description of changes in the system and define inter-relationship between its elements.

Prior efforts to comprehensively identify and evaluate potential factors that contribute to the aging process have benefited from microarray analysis. Multiple studies have addressed the effect of aging on the transcriptional level in different tissues, including skeletal muscle in the leg (gastrocnemius) of mice [5], mouse brain [6], human and mouse kidney [7,8]. However, it has been found that the correlation between mRNA abundance and the quantity of the corresponding functional protein present within a cell is rather poor [9], therefore transcriptomic information alone is not sufficient to clarify the mechanism of aging.

Proteomics technology is an approach to examine and identify protein dynamics of biological pathways and multifactorial disease processes. Because these techniques can analyze the final end products of genes, they provide more functional insight. During the last decade a number of proteomic gel-based studies on aging tissues have been performed: 2-DE study of aging brain in mice [10], human normal colon epithelia [11], aging mouse kidney [8] among others. These studies reported on average up to 50 proteins with significant differential expression in old tissues compared to young. It has been observed that consequences of aging are tissue-specific

Abbreviations: ROS, reactive oxygen species; ESI, electrospray; LC–MS/MS, liquid chromatography–tandem mass spectrometry; PCA, principle component analysis.

* Corresponding author. Tel.: +46 8 16 2378; fax: +46 8 15 3679.
E-mail address: hanna.amelina@dbb.su.se (H. Amelina).

1570-0232/$ – see front matter © 2011 Elsevier B.V. All rights reserved.
doi:10.1016/j.jchromb.2011.08.044

[12,13], which may be due to the organs' differing regenerating activity. For instance liver has a remarkable capacity to regenerate after injury, compared to other organs such as kidney and brain that undergo irreversible functional decline.

Recently a great progress in the field of high-resolution shotgun mass spectrometry-based proteomics has been made, allowing for accurate identification and quantification of complex protein samples. These techniques have already been applied to study age-related changes in biological systems, and one of such examples is a quantitative proteomic profiling of age-related changes of human cerebrospinal liquid using ICAT and mass spectrometry [14]. Another recent study from M. Mann laboratory [15], in which SILAC metabolic labeling of mice has been utilized to examine changes of the mouse tissue proteomes during aging, surprisingly reported only few proteins that differentially expressed with age.

In the present study, iTRAQ-based quantitative proteomic approach has been utilized to investigate the changes in the liver proteome during the age course. In order to reduce sample complexity and the masking effect of highly abundant proteins we have focused on peroxisome-enriched fractions.

Peroxisomes are important cell organelles involved in oxidative metabolism in nearly all eukaryotes. They harbor enzymes involved into a variety of essential metabolic processes, such as β-oxidation of long-chain fatty acids and the synthesis of ether lipids in men [16]. Peroxisomes contain hydrogen peroxide producing oxidases and hence, contribute to the cellular production of reactive oxygen species (ROS) that accumulate with age and can damage important macromolecules such as DNA, proteins and lipids.

Until recently mitochondria were considered a key player in ROS generation, and their role in aging has been addressed in a number of proteomic studies [17–19]. However, soon it became evident that in specific cells or tissues (e.g. liver) peroxisomes represent major ROS producers. Moreover, peroxisomal dysfunction has been shown to be associated with cellular aging and molecular pathologies that often lead to age-related degenerative diseases [20,21]. These facts altogether make peroxisomes another appealing organelle for studying the mechanisms of aging.

In our study we applied a mass spectrometry-based quantitative proteomic method to explore how aging affects the peroxisomes. Here, we show that the peroxisomal proteome of mouse liver undergoes only slight changes during aging, and that inter-individual variation must be considered in aging studies.

2. Materials and methods

2.1. Chemicals

Optiprep was purchased from Axis-Shield, Norway. Complete Protease Inhibitor Cocktail was from Roche Diagnostics, Mannheim, Germany. Anti-catalase antibody was purchased from Rockland Immunochemicals, Inc.; anti-prohibitin (H-80) and anti-epoxide hydrolase (A-5) antibodies were from Santa Cruz Biotechnology, Inc. iTRAQ reagents and trypsin were from Applied Biosystems AB (Foster City, CA). 3-(N-morpholino) propanesulfonic acid (MOPS), acetonitrile (ACN), formic acid (FA) and acetic acid (HAc) were obtained from Merck (Darmstadt, Germany). Sucrose, EDTA and urea were from Sigma–Aldrich (St. Louis, MO, USA). All water used was Milli-Q ultra-pure (Millipore, Bedford, MA, USA).

2.2. Animals

Frozen livers from male C57BL6/J mice of 10-week-old and 18-month-old were purchased from Janvier laboratories (Le Genest-St-Isle, France). Livers from six biological replicates per age group were used in this study. Organs were dissected according to standard protocols, snap-frozen in liquid nitrogen and air-transported with dry ice on the same day.

Table 1
Experimental design.

Experimental run order	Labels			
	114	115	116	117
1	pool	young 1	young 2	old 1
2	pool	old 2	old 3	young 3
3	pool	young 4	young 5	old 4
4	pool	old 5	old 6	young 6

2.3. Cell fractionation and isolation of peroxisome-enriched fraction

Frozen tissues were thawed on ice, minced and homogenized in the ice-cold homogenization buffer (250 mM sucrose, 5 mM MOPS, 0.5 M EDTA, 0.1% ethanol) in the presence of Complete Protease Inhibitor Cocktail (1 tablet dissolved in 50 mL buffer). Four individual livers that included samples from both age groups were processed simultaneously, enabling us to reduce possible "batch effect". The subcellular fractionation by differential and density centrifugation was performed as described previously [22] with a few modifications outlined below. The main subcellular fractions were termed according to the nomenclature used by Volkl and Fahimi [23]. Thus, the crude homogenate was termed A, the heavy mitochondrial fraction was termed B, postmitochondrial faction was termed C, the light mitochondrial or peroxisome-enriched fraction was termed D, the cytosolic fraction was termed E, and the microsomal was termed F. Two milliliters of the resuspended D fraction were carefully layered on the top of 10 mL of 28% iodixanol (v/v), 5 mM MOPS, 0.1% ethanol, 1 mM EDTA solution and 1 mL of 50% iodixanol cushion and centrifuged at 131,000 g_{av} for 2 h. The peroxisome-enriched fractions were collected from the interface between 28 and 50% iodixanol. The efficiency of purification procedure was assessed using protein immunoblot against peroxisomal catalase and mitochondrial prohibitin (Fig. 1). Protein concentration in obtained fractions was determined according to Bradford [24]. The fractions corresponding to 90 μg of proteins were then freeze-dried and then processed according to the iTRAQ reagents protocol (Applied Biosystems AB). As none of the substances present in the homogenization buffer were listed as interfering with the iTRAQ reagents protocol, protein precipitation step prior digestion was omitted in order to minimize protein losses.

2.4. Experimental design

The samples were divided into four 4-plex experiments (Table 1), and a pooled reference sample prepared by combining aliquots from 6 young and 6 old samples, was incorporated into each experiment. This experimental setup enabled us to simultaneously analyze the data across the four 4-plex experiments, and to correct for experimental variability across multiple experiments. For every 4-plex experiment equivalent amount of protein from each biological replicate and pooled reference sample was reduced, alkylated, digested and labeled with one of the isobaric tags. The reference standard was allocated into each experiment using the same labeling tag, and the rest of samples were allocated to the remaining tags.

2.5. Protein reduction, alkylation and trypsin digestion

Protein denaturation, reduction, cysteine blocking and digestion were performed according to the protocol provided by the

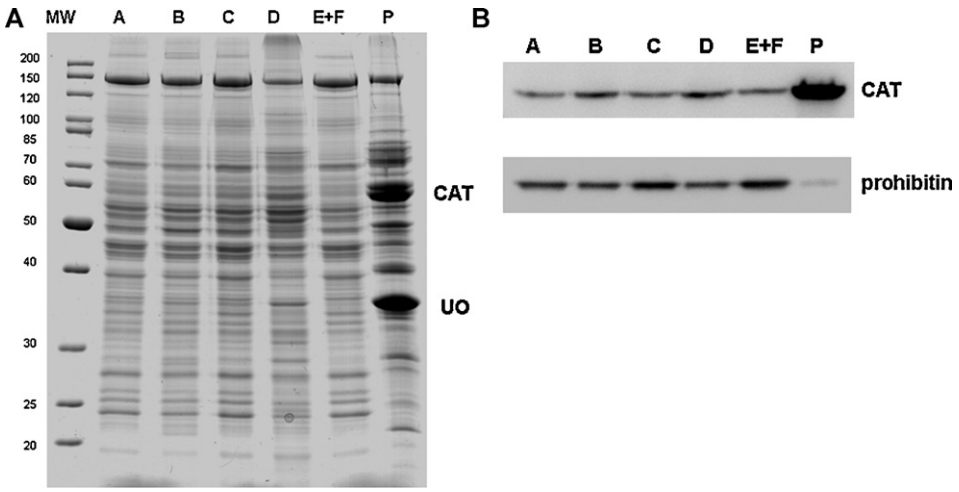

Fig. 1. SDS-PAGE (A) and immunoblotting (B) of different subcellular fractions from the peroxisomes enrichment procedure. A – postnuclear fraction, B – mitochondrial fraction, C – postmitochondrial fraction, D – light mitochondrial fraction, E + F – microsomal + cytosolic fraction, P – peroxisome-enriched fraction. CAT – catalase; UO – urate oxidase.

manufacturer (Applied Biosystems, Foster City, CA) with a few modifications outlined below. Briefly, freeze-dried samples were resuspended in 20 μL of Dissolution Buffer (0.5 M triethyl ammonium bicarbonate buffer (TEAB) pH 8.5), 1 μL of denaturant (1 M urea) was added to denature the samples and assist dissolution. The proteins then were reduced with 5 mM tris(2-carboxyethyl) phosphine (TCEP) for 1 h at 37 °C and alkylated with 10 mM S-Methyl methanethiosulfonate (MMTS) for 10 min at room temperature. 10 μL of trypsin solution (10 μg/μL) was added to each sample and the digestion was performed for 18 h at 37 °C.

2.6. Labeling the protein digests with iTRAQ reagents

Digested samples were labeled with the iTRAQ reagents following the protocol provided by the vendor (Applied Biosystems, Foster City, CA). In brief, the iTRAQ reagents reconstituted in 70 μL of ethanol were added to each sample containing 90 μg of protein, and the labeling was carried out for 1 h at room temperature. The labeled digests corresponding to each of the four 4-plex experiments were combined and dried using rotary vacuum concentrator.

2.7. Sample desalting and nano-LC–ESI-MS/MS analysis

The digested sample was diluted to a volume of 500 μL with 2.5% HAc (v/v) and desalted on a Isolute C18(EC) (1 mL, 50 mg capacity, Biotage, Uppsala, Sweden) SPE column using the following scheme: the column was first wetted with 5 mL 100% ACN and equilibrated with 5 × 1 mL 1% HAc. The tryptic peptides were adsorbed to the media using 5 repeated cycles of sample loading. The column was washed using 5 × 1 mL of 1% HAc and finally the peptides were eluted in 400 μL 50% ACN, 1% HAc. The aliquots were vacuum centrifuged to dryness, followed by reconstitution in 540 μL of buffer (solvent A: H_2O/ACN/FA 97.9/2/0.1, v/v%).

The separation was performed using a Tempo nanoLC-1D plus™ (AB Sciex, USA) system. A volume of 3 μL of each sample was injected into a 10 μL loop in injection pickup mode. The samples were loaded onto a Peptide CapTrap (Michrom Bioresources, CA, USA) for 5 min at 15 μL/min isocratically (solvent A: H_2O/ACN/FA 97.9/2/0.1, v/v%). The peptides were then eluted onto a BioBasic-C18 column 5 μm × 15cm × 75 μm (Thermo) using a stepwise gradient (solvent A; solvent B: H_2O/ACN/FA 2/97.9/0.1, v/v%) at a flow rate of 350 nL/min. The gradient was as follows (% solvent B in A/min): 2/0, 2/20, 8/25, 32/100, 40/115, 80/116, 80/120, 2/125, 2/139. The samples were kept in the autosampler at 10 °C. Data was collected in positive ESI mode on a hybrid quadrupole/time-of-flight (Q/TOF) Qstar XL™ operated with the Analyst QS v1.1 software (AB Sciex). The ion source was a MicroIonSpray II® head with an uncoated 10 μm i.d. PicoTip® (New Objective, MA, USA) as electrode. The source parameters were: ion spray voltage, 2200 V; curtain gas, 20 psi; gas 1, 15 psi; interface heater temperature, 125 °C and the ions were drawn into the first quadrupole by a declustering and focusing potential of 60 and 230 v respectively. Information dependent acquisition (IDA) was employed in which each cycle consisted of a survey scan from *m/z* 400 to 1600 (0.5 s) followed by MS/MS from *m/z* 65 to 1600 (1.5, 2.0, 2.5 s) of the three ions that exhibited the highest signal intensity. In the survey scan, the ions were guided through the quadrupoles operating in RF-only and orthogonally guided, accelerated and analyzed by the TOF. In MS/MS mode, the first quadrupole was employed to filter one selected ion (the precursor window was set to low), while the second quadrupole operated as a collision cell followed by spectrum acquisition using the TOF. Collision voltages were automatically adjusted based on the ion charge state and mass using rolling collision energy of the filtered peptide ion. MS/MS was only triggered for ions of charge state 2–4 exceeding an intensity of 20 counts and were excluded for fragmentation for 60 s after one MS/MS spectra.

2.8. Data analysis

Protein identification was carried out using ProteinPilot™ Software v.3.0 (Applied Biosystems, Foster City, CA). A Paragon algorithm [25] in ProteinPilot™ Software was used as the default search program. Parameters, such as tryptic cleavage specificity, precursor ion mass accuracy and fragment ion mass accuracy, are in-built functions of Protein Pilot software. The Paragon algorithm was set up to search for iTRAQ-labeling modifications on the N-termini of peptides and the side chains of lysine and tyrosine as variable modifications, and alkylation of cysteines by MMTS as a fixed modification. One missed cleavage site was allowed. The database search was set up to a "thorough" search against UniProtKB/Swiss-Prot Release 51.6 database. For successful protein identifications, at least one peptide with unique sequence was required. The Protein Pilot algorithm was selected to search automatically for biological modifications, the confidence level for protein identification was set to 1.3 (95%). Relative quantification of proteins using ProteinPilot is performed on the MS/MS scans and is calculated based on the ratio of the areas of the 114-, 115-, 116-, and 117-Da iTRAQ reporter ions. ProteinPilot calculates average

protein ratios using only ratios from the spectra that are distinct to each protein, excluding the shared peptides of isoforms.

The protein list from 4 iTRAQ experiments were merged with ratios calculated to a global standard 114. Two-sided *t*-tests were carried out after filtering for proteins present (or quantified) in three out of six samples under the assumption of equal variance between age groups. All protein iTRAQ ratios were transformed to natural logarithmic scale and those values were used for calculation of the *p*-values. Proteins with *p*-values less than 0.05 were considered as expressed at significantly different levels. Geometric means for each spot and age group were calculated; using those values, fold changes between two ages were obtained, and the values were transformed to base 2 logarithm values. In base 2 logarithm space, a two-fold change in levels is reported as −1 or 1 in case of down-regulated and up-regulated changes respectively. Using $\log_2$-transformed values, standard deviations for each protein were calculated in order to assess the inter-individual variability between samples within each age group.

Using MiniTab 16 statistical software, principle component analysis (PCA) was performed to visualize the relative location of each individual sample in a two-dimensional space, allowing the detection of outliers or other relevant patterns such as inter-individual variation and group separation based on the selected set of variables. A correlation matrix where each protein was set as a variable and each biological replicate as an observation was used to extract the principle components. For the proteins that were found to be differentially expressed according to the *t*-test ($p < 0.05$) boxplot graphs were created with help of MiniTab 16.

2.9. Western blot validation of iTRAQ mass spectrometry results

In order to validate some of our findings, we conducted immunoblotting using antibodies against selected proteins (epoxide hydrolase 2, alpha-amylase and 2,4-dienoyl-CoA reductase), following standard procedures and using chemoluminescence for detection. These three proteins were chosen based on the commercial availability of antibodies, fold-changes levels detected by iTRAQ–MS/MS (i.e. proteins with relatively high fold-changes were selected), as well as expected protein abundance in the fractions examined.

3. Results and discussion

3.1. Overview of subproteome isolation and experimental design considerations

Tissues were subjected to conventional differential centrifugation and the peroxisome-enriched fractions were purified with iodixanol gradient using density-gradient centrifugation as described in Section 2. The quality of this procedure was assessed by Western blotting against common organelle markers. As illustrated in Fig. 1, the subcellular fractionation method applied here clearly resulted in strong enrichment of the peroxisomal marker catalase and concomitant depletion of the mitochondrial marker prohibitin.

In our study we have used a reference sample pooled from an aliquot of each sample (both ages), that was incorporated into each of the four iTRAQ experiments. Presence of the common internal standard enabled us to perform comparison between multiple samples between and within age groups. To assess biological variation, individual samples were labeled independently instead of pooling and labeling biological specimens from the same age group. We observed a high biological variability between individuals (Fig. 2) that was in some cases more pronounced than changes induced by aging (Fig. 3). This finding was rather surprising considering that an inbred mouse strain with matching genetic background was used.

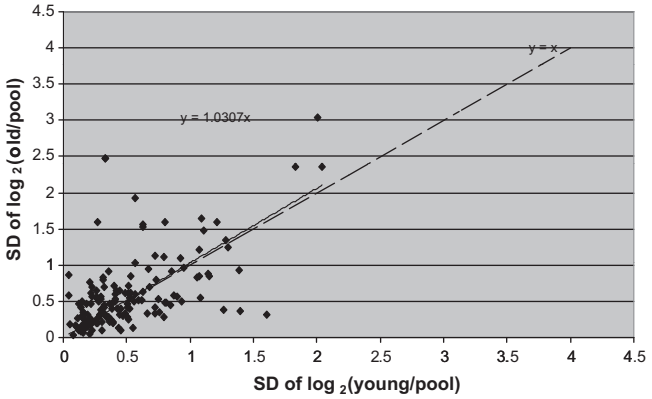

Fig. 2. Comparison of standard deviation values SD ($\log_2$) for 150 proteins from young samples against old ones.

3.2. Statistical analysis of mass spectrometry data

A representative mass spectrum of one of the proteins identified and quantified in this study is depicted in Fig. 4.

Merging the datasets from four iTRAQ experiments led to the identification of 234 proteins. Out of all identified proteins, 150 (64%) were identified and quantified in at least three biological replicates out of the six that were used in the study. Hence, only those 150 proteins were subjected to further statistical analysis. Unprocessed data from the independent iTRAQ experiments before the data was merged can be found in Supplementary files 1–4. Missing values in the data set came from the cases when proteins were identified but not quantified, or when a protein was absent in the analyzed sample.

To uncover proteins that were differently expressed in two ages we have used a two-tailed paired *t*-test with a *p*-value cutoff of 0.05. Only eight proteins showed statistical significance according to the *t*-test performed (Table 2, Fig. 5). At the same time, 31 proteins out of 150 considered in the analysis, had a fold change above 1.4 ($\log_2 < \pm 0.485$), but only 6 of them were significantly different expressed according to the *t*-test. iTRAQ ratios obtained from the merged datasets and details on the statistical analysis that has been performed are provided in Supplementary file 5.

Using MiniTab statistical software multivariate analysis of the data was conducted. First we performed PCA using all the proteins that were identified and quantified at least in 50% of all biological replicates within an age group (present in 3 out of 6 biological replicates in each age group). Two first principle components explained 43.7% of the total variation, and five first principle components – 74.1% (Fig. 6A). It has to be mentioned that the distances between the samples of the same age group generally were not smaller than those between the samples of different age groups. As a next step we performed PCA using 8 proteins that were differentially expressed between two ages according to the statistical analysis (Fig. 6B). In this case 61.9% of the variation was explained by the first component, and two first components determined 74.5% of the total variation. First component was able to separate the young samples from the old ones based on the differences in their proteomes. Noteworthy, the distance between samples from 10-week-old mice was generally shorter than the distance between 18-month-old samples.

Similar results were obtained when two samples of the same age (Fig. 3A and B) and two samples from different age groups (Fig. 3C)

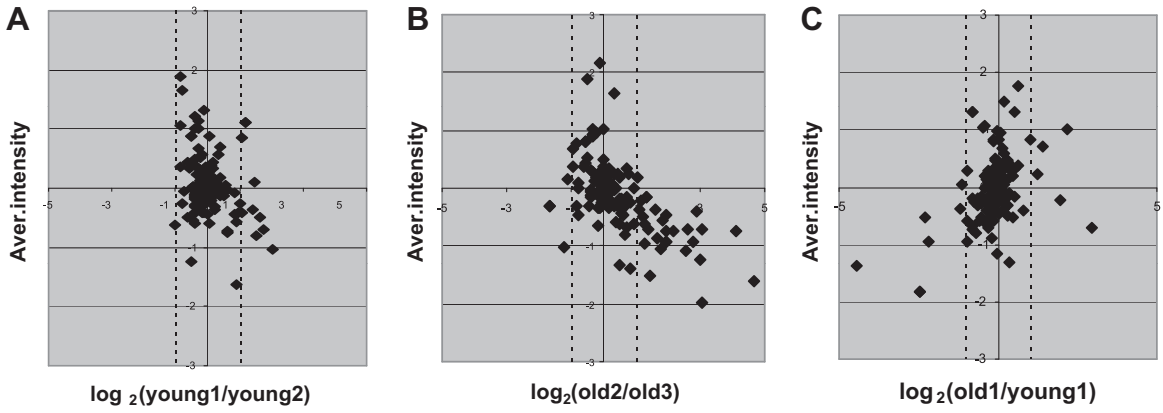

Fig. 3. Intensity-ratio distribution of protein abundances. The *x*-axis shows the logarithm (base 2) of the ratios; the *y*-axis corresponds to the average intensity of the logarithms of the ratios. Vertical bias trend line corresponds to $x = 1$ (which equals to $\log_2(2)$ and represents two-fold ratio). (A) and (B) Comparison between two biological replicates, (C) comparison between an old and a young animal.

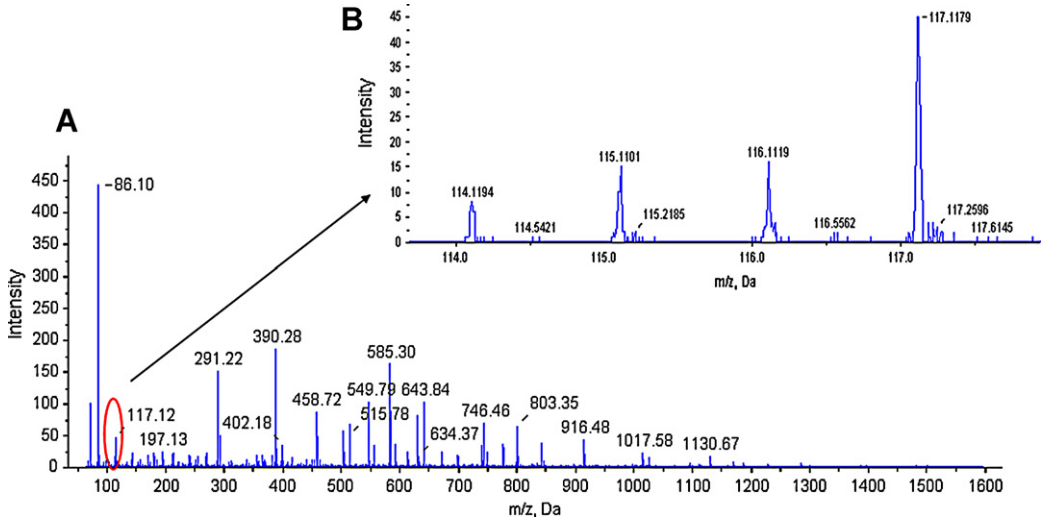

Fig. 4. (A) A representative MS/MS spectrum of the peptide DTTPDELLSAVLTAVLQDVK[IT4] from 3-keto-acyl CoA thiolase, peroxisomal (precursor ion [M+3H]3+, Mr = 2415.3 Da). [IT4] indicates any of the 4-iTRAQ labels. (B) The iTRAQ reagent quantitation region showing the reporter ions for the peptide.

were randomly selected for comparison. The results are presented in graphs as a function of average intensity of reporter ion ratios (Fig. 3). As it can be seen in Fig. 3A, samples from 10-week-old group (young) are characterized by more similar protein expression pattern compared to those from 18-month-old mice (old) (Fig. 3B). Moreover, differences in protein expression between the samples originating from two different age groups (Fig. 3C) are comparable with those between two samples of older age, that were caused by inter-individual variability. Therefore we suggest that the rather low number of differentially expressed proteins uncovered in this study may be due to a high biological variability, particularly in the case of old animals.

3.3. *Identification of proteins differentially expressed in peroxisome-enriched fraction in mouse liver with age*

In this study we performed comparative analysis of liver subproteome from young and old mice, which led to identification and relative quantitation of 8 differentially expressed proteins. Compared to the young mice, four peroxisomal proteins were significantly overexpressed in the old-age liver proteome. Among these, epoxide hydrolase 2 was approximately 1.6-fold up-regulated in old mice compared to the young. Epoxide hydrolase, localized in both the cytosol and peroxisomes, binds to specific epoxides and converts them to less toxic and readily excretable

Table 2
Proteins differentially expressed with age (according to the *t*-test, $p < 0.05$).

No.	Protein name	Accession number	Subcellular localization	*p*-value	Fold change	Up/down-regulation
1	Epoxide hydrolase 2	sp|P34914	pero/cyto	0.019	1.6	up
2	3-ketoacyl-CoA thiolase A, peroxisomal	sp|Q921H8	pero	0.004	1.4	up
3	Peroxisomal sarcosine oxidase	sp|Q9D826	pero	0.023	1.2	up
4	Pancreatic alpha-amylase	sp|P00688	lyso	0.021	−4.1	down
5	Peroxisomal 2,4-dienoyl-CoA reductase	sp|Q9WV68	pero	0.048	1.7	up
6	Prohibitin-2	sp|O35129	mito	0.011	1.3	up
7	Cytochrome c oxidase subunit 6 C	sp|Q9CPQ1	mito	0.003	−1.6	down
8	Cytochrome b-c1 complex subunit 2, mitochondrial	sp|Q9DB77	mito	0.027	−1.6	down

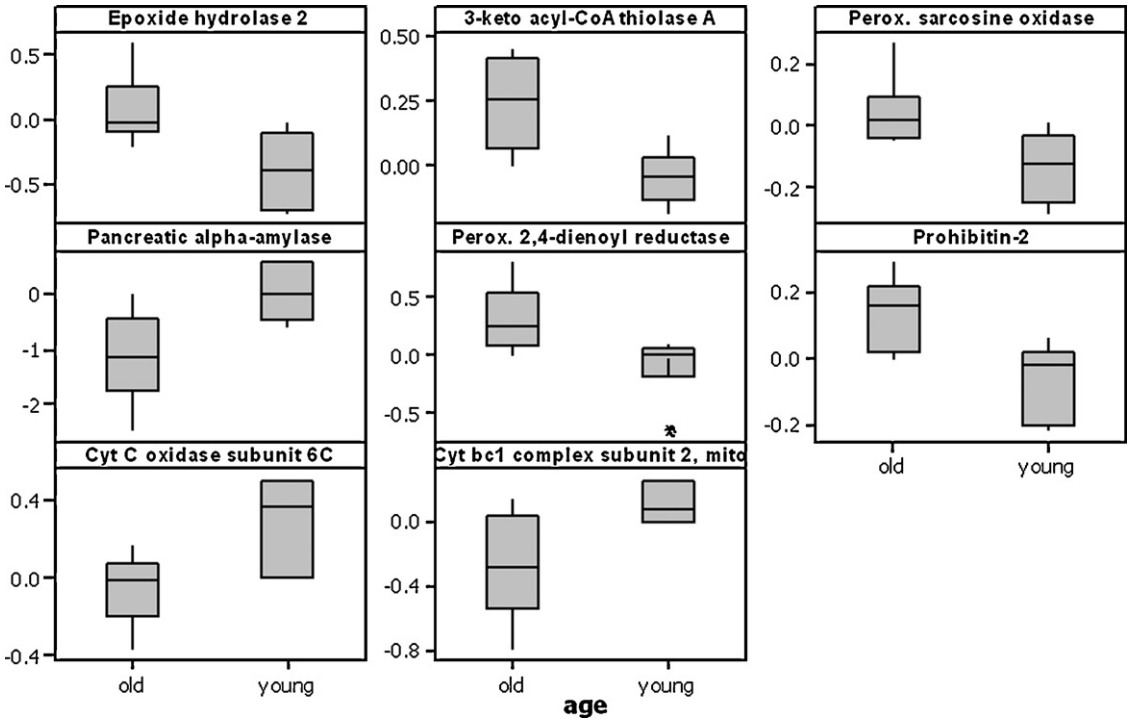

Fig. 5. Boxplots for the 8 proteins differentially expressed between two ages. The band near the middle of the box corresponds to the median. The lower and higher whiskers represent the lowest and highest observations. Extreme observations are plotted with asterisks (*).

dihydrodiols. The up-regulation of this protein, observed in elderly mouse liver may indicate an adaptive process of the liver to counteract the adverse effects of aging process.

Additionally, we performed Western blot analysis using monoclonal antibodies against epoxide hydrolase 2 to validate this finding, and detected 1.4-fold age-related up-regulation of epoxide hydrolase, which correlated fairly well with 1.6-fold that was detected by iTRAQ–MS/MS (Fig. 7).

Another peroxisomal protein that was significantly up-regulated in aged liver with a fold of 1.4 was 3-ketoacyl-CoA thiolase A. This protein is involved in the β-oxidation process, where it catalyzes the final step, in which a two-carbon unit is cleaved from the fatty acid. The increased levels of 3-ketoacyl-CoA thiolase A mRNA in aging rat liver has been previously reported in transcriptomic analysis using cDNA microarray [26], as well as in immunoblotting study [27]. Since peroxisomal β-oxidation of fatty acids is known to decrease with age, it would not provide explanation to the increase of 3-ketoacyl-CoA thiolase A observed in our study. However it is now known that rat liver peroxisomes participate in cholesterol biosynthesis, and peroxisomal thiolase is responsible for the initial step in this process, the condensation of acetyl-CoA units into acetoacetyl-CoA [28]. Therefore augmentation of peroxisomal 3-ketoacyl-thiolase A with aging can be related to the increased level of cholesterol in aged rats.

Another peroxisomal protein that was up-regulated with aging, although with only 1.2-fold, was sarcosine oxidase. This protein catalyzes oxidative demethylation of sarcosine to yield glycine, formaldehyde and hydrogen peroxide. Sarcosine oxidase is also known to be involved in the oxidation of L-proline and pipecolic acid. Belonging to a pool of peroxisomal oxidases, sarcosine oxidase

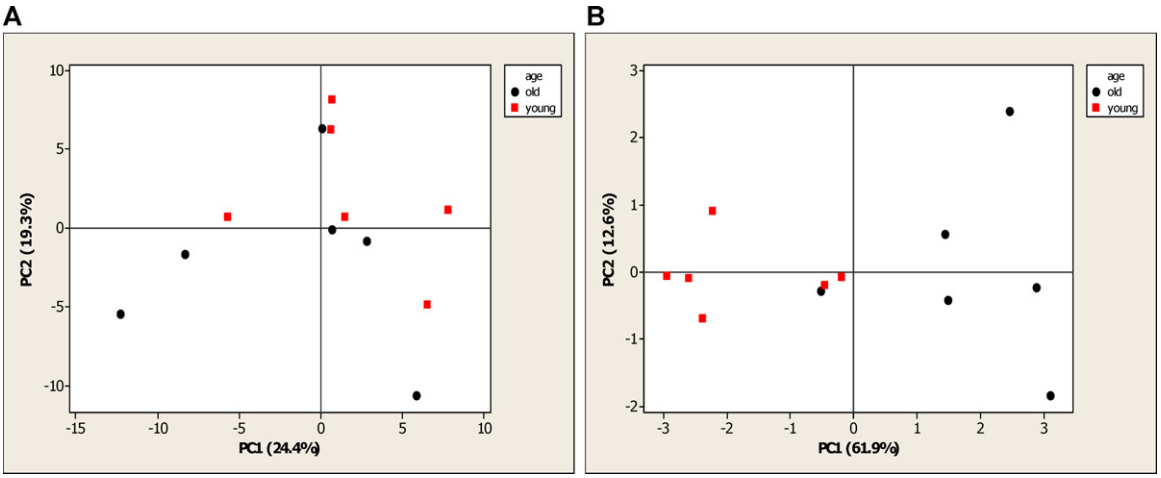

Fig. 6. Principle Component Analysis score plots: (A) PCA for 150 proteins (variables) from 12 samples (observations) were analyzed, the first two components explained 43.7% of variance; (B) PCA of 8 proteins from 12 samples that were found to change significantly following the *t*-test (*p*-value <0.05). First two components explained 74.5% of variance.

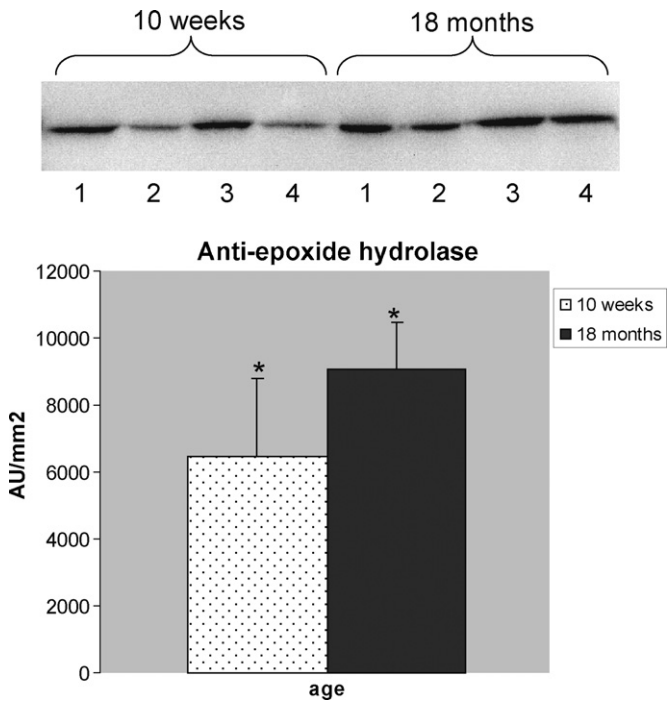

Fig. 7. Validation of age-related expression level of epoxide hydrolase 2 by Western immunoblotting. 30 μg of protein per lane was loaded. Four biological replicates were used per each age-group.

contributes to ROS production by generation of hydrogen peroxide. Therefore statistically significant albeit slight increase in the expression of sarcosine oxidase observed in our study, is in agreement with the "oxidative damage" theory of aging.

Finally, we observed age-related significant up-regulation of peroxisomal 2,4-dienoyl-CoA reductase (DECR). This protein is an auxiliary enzyme of β-oxidation that belongs to a family of short-chain dehydrogenases/reductases (SDR). It participates in the degradation of unsaturated fatty enoyl-CoA esters that have double bonds in both even- and odd-numbered positions. As mentioned above, peroxisomal β-oxidation of fatty acids decreases with age. It has been proposed that decreased activity of acyl-CoA oxidase is the limiting step in the degradation of unsaturated fatty acids, therefore the up-regulation of other enzymes in the β-oxidation pathway would not result in the increased level of peroxisomal β-oxidation. Therefore we believe that up-regulated expression of DECR in old mice detected in our study may indicate an adaptive response if the peroxisomal enzyme to counteract age-related decrease in the efficiency of β-oxidation. Additionally we performed Western blotting analysis in attempt to validate our finding, but were not able to detect any signal.

Additionally, among the proteins differentially expressed with age, we identified three mitochondrial proteins. It has to be mentioned that even though the presence of mitochondrial proteins in the given study represents a contamination, the reproducibility of peroxisome-enriched fraction isolation has been repeatedly tested in our group in previous studies [29–31].

Among mitochondrial proteins differentially expressed in mouse liver subproteome with age, we identified prohibitin-2. This protein constitutes one of the subunits of prohibitin complex that assemble at the inner mitochondrial membrane, and it has been suggested that it might be involved in regulating mitochondrial respiration activity. Prohibitin complex is known to inhibit cell proliferation and apoptosis, therefore it has been proposed that it can promote longevity by moderating fat metabolism, mitochondrial proliferation and energy levels [32]. The slight decrease in prohibitin observed in our study may indicate an adaptive response of liver proteome to the aging process. In support of our hypothesis, increase of prohibitin has been reported in another study, where effect of aging on mitochondrial proteome in rats was evaluated using 2-DE PAGE [33].

In total three proteins were found to be down-regulated with age in the present study. Among them two mitochondrial proteins have been identified: cytochrome c oxidase subunit 6C and subunit 2 of cytochrome b-c1 complex.

The activity of cytochrome c oxidase, which is the terminal component of the mitochondrial electron transport chain, has been previously reported to significantly decrease with age in insects and mammals [34]. This decline has been shown to correlate with the concomitant increase in the amount of ROS, such as hydrogen peroxide and superoxide anion. Hence, the decrease in the amount of cytochrome c oxidase subunit observed in our study, appears to support the "oxidative damage" theory of aging.

Cytochrome b-c1, the third complex in the electron transport chain (ETC) in mitochondria, operates through a Q-cycle mechanism that couples electron transfer to generation of the proton gradient that drives ATP synthesis. Cytochrome b-c1 complex is generally thought to generate superoxide anion that participates in cell signaling and contributes to cellular damage in aging and degenerative diseases. It has been previously reported that aging caused decrease in activity of complex III in intrafibrillar mitochondria in the elderly rat hearts [35], however no proteomic studies have previously reported the decrease in the amount of the subunits of complex III. Aging related alterations in complex III are likely to enhance the production of ROS due to the increased relative reduction of cytochrome b and the generation of ROS via electron leak from the cytochrome b.

Finally, we have identified pancreatic alpha-amylase that was down-regulated in the old age group with the highest fold change observed in this study (4.1). This enzyme with predicted lysosomal localization, catalyzes the cleavage of alpha-1,4-glucosidic linkages between glucose molecules in starch, and thus plays an important role in starch digestion. It has been shown for parotid and other exocrine glands that synthesis of secretory proteins, especially alpha-amylases, declines with age, and the salivary function in general decreases [36]. This observation would explain significant decrease of alpha-amylase level in old mouse liver that we observe in our study. However, there are more recent contradictory results from cDNA microarray studies that reported increased levels of alpha-amylases in heart, liver and hypothalamus of aged mice [37].

Additionally, we attempted to validate this result using Western immunoblotting with anti-alpha-amylase monoclonal antibodies, but unfortunately could not detect any signal, most probably due to the low abundance of alpha-amylase protein in our fraction of interest.

4. Conclusions

In conclusion, we have applied a subproteomic approach based on iTRAQ quantification to study the effect of aging on mouse liver peroxisomes. Statistical analysis allowed discriminating eight proteins that were differentially expressed with age at a significant level. Most of the proteins identified are related to the ROS production/breakdown, which supports "the free-radical theory of aging". Our results indicate that the expression levels of the majority of the proteins undergo only slight changes during aging. However, as our data represents averages obtained from a limited number of biological replicates, rather few differentially expressed proteins identified may be also explained by a high inter-individual variability. One possible way to increase the reliability of the data in such kind of studies would be to increase the number of

biological replicates, which unfortunately very often stands as a limiting factor in aging research.

Nevertheless, our study shows that shotgun quantitative proteomics is a useful tool that is able to complement traditional genomic and transcriptomic approaches and can provide new insight into the cellular mechanisms of aging.

Acknowledgements

This work was supported by grants from the Swedish Research Council – Medicine and Swedish Research Council – Natural Science (VR-M and VR-N), Carl Trygger Foundation, VINNOVA – Vinnmer program, Magnus Bergvalls Foundation, Oscar and Lilli Lamms Minne Foundation, IKERBASQUE, CBR-SSF.

We thank Jan-Olov Persson from the Division of Mathematical Statistics, Stockholm University for his advice regarding statistical analysis of the data.

Appendix A. Supplementary data

Supplementary data associated with this article can be found, in the online version, at doi:10.1016/j.jchromb.2011.08.044.

References

[1] A.G. Ryazanov, B.S. Nefsky, Mech. Ageing Dev. 123 (2002) 207.
[2] M.W. Djojosubroto, Y.S. Choi, H.W. Lee, K.L. Rudolph, Mol. Cells 15 (2003) 164.
[3] A. Morley, Ann. N. Y. Acad. Sci. 854 (1998) 20.
[4] T. Dimauro, G. David, Aging (Albany NY) 1 (2009) 182.
[5] R. Weindruch, T. Kayo, C.K. Lee, T.A. Prolla, J. Nutr. 131 (2001) 918S.
[6] T.A. Prolla, Chem. Senses 27 (2002) 299.
[7] A. Melk, E.S. Mansfield, S.C. Hsieh, T. Hernandez-Boussard, P. Grimm, D.C. Rayner, P.F. Halloran, M.M. Sarwal, Kidney Int. 68 (2005) 2667.
[8] H. Amelina, S. Cristobal, Proteome Sci. 7 (2009) 16.
[9] L. Anderson, J. Seilhamer, Electrophoresis 18 (1997) 533.
[10] O. Carrette, P.R. Burkhard, D.F. Hochstrasser, J.C. Sanchez, Proteomics 6 (2006) 4940.
[11] M. Li, Z.Q. Xiao, Z.C. Chen, J.L. Li, C. Li, P.F. Zhang, M.Y. Li, J. Biochem. Mol. Biol. 40 (2007) 72.
[12] J. Mi, I. Garcia-Arcos, R. Alvarez, S. Cristobal, Proteome Sci. 5 (2007) 19.
[13] M.E. Dolle, W.K. Snyder, J.A. Gossen, P.H. Lohman, J. Vijg, Proc. Natl. Acad. Sci. U.S.A. 97 (2000) 8403.
[14] J. Zhang, D.R. Goodlett, E.R. Peskind, J.F. Quinn, Y. Zhou, Q. Wang, C. Pan, E. Yi, J. Eng, R.H. Aebersold, T.J. Montine, Neurobiol. Aging 26 (2005) 207.
[15] D.M. Walther, M. Mann, Mol. Cell. Proteomics 10 (2011) M110004523.
[16] H. van den Bosch, R.B. Schutgens, R.J. Wanders, J.M. Tager, Annu. Rev. Biochem. 61 (1992) 157.
[17] A.N. Kiri, H.C. Tran, K.L. Drahos, W. Lan, D.K. McRorie, M.J. Horn, J. Biomol. Tech. 16 (2005) 371.
[18] K. O'Connell, K. Ohlendieck, Proteomics 9 (2009) 5509.
[19] N.A. Dencher, S. Goto, N.H. Reifschneider, M. Sugawa, F. Krause, Ann. N. Y. Acad. Sci. 1067 (2006) 116.
[20] S.R. Terlecky, J.I. Koepke, P.A. Walton, Biochim. Biophys. Acta 1763 (2006) 1749.
[21] J.I. Koepke, C.S. Wood, L.J. Terlecky, P.A. Walton, S.R. Terlecky, Toxicol. Appl. Pharmacol. 232 (2008) 99.
[22] M.K. Ghosh, A.K. Hajra, Anal. Biochem. 159 (1986) 169.
[23] A. Volkl, H.D. Fahimi, Eur. J. Biochem. 149 (1985) 257.
[24] M.M. Bradford, Anal. Biochem. 72 (1976) 248.
[25] I.V. Shilov, S.L. Seymour, A.A. Patel, A. Loboda, W.H. Tang, S.P. Keating, C.L. Hunter, L.M. Nuwaysir, D.A. Schaeffer, Mol. Cell. Proteomics 6 (2007) 1638.
[26] P. Tollet-Egnell, A. Flores-Morales, N. Stahlberg, R.L. Malek, N. Lee, G. Norstedt, Mol. Endocrinol. 15 (2001) 308.
[27] K. Beier, A. Volkl, H.D. Fahimi, Virchows Arch. B Cell. Pathol. Incl. Mol. Pathol. 63 (1993) 139.
[28] S.L. Thompson, S.K. Krisans, J. Biol. Chem. 265 (1990) 5731.
[29] J. Mi, A. Orbea, N. Syme, M. Ahmed, M.P. Cajaraville, S. Cristóbal, Proteomics 5 (2005) 3954.
[30] I. Apraiz, J. Mi, S. Cristobal, Mol. Cell. Proteomics 5 (2006) 1274.
[31] J. Mi, E. Kirchner, S. Cristobal, Proteomics 7 (2007) 1916.
[32] M. Artal-Sanz, N. Tavernarakis, Nature 461 (2009) 793.
[33] J. Chang, J.E. Cornell, H. Van Remmen, K. Hakala, W.F. Ward, A. Richardson, J. Gerontol. A Biol. Sci. Med. Sci. 62 (2007) 223.
[34] R.S. Sohal, D. Toroser, C. Bregere, R.J. Mockett, W.C. Orr, Mech. Ageing Dev. 129 (2008) 558.
[35] E.J. Lesnefsky, T.I. Gudz, S. Moghaddas, C.T. Migita, M. Ikeda-Saito, P.J. Turkaly, C.L. Hoppel, J. Mol. Cell. Cardiol. 33 (2001) 37.
[36] S.K. Kim, L.M. Cuzzort, R.K. McKean, Arch. Oral Biol. 37 (1992) 349.
[37] C. Fu, M. Hickey, M. Morrison, R. McCarter, E.S. Han, Mech. Ageing Dev. 127 (2006) 905.